A control scheme for the tracking control of the Furuta pendulum*

Carlos Aguilar–Avelar and Javier Moreno–Valenzuela**

Instituto Politécnico Nacional–CITEDI,
Av. del Parque 1310, Mesa de Otay, Tijuana, B.C., Mexico
{caguilar, moreno}@citedi.mx
http://www.citedi.mx
Paper received on 24/09/12, Accepted on 25/10/12.

Abstract. The purpose of this document is to introduce a new control scheme which is based in the feedback linearization technique. The error signal is defined as a vector of dimensation two, with first element defined as the difference between a differentiable time–varying signal and the arm position, while the second element is defined as the negative of the pendulum position. The control problem consists in designing a control input to keep the error trajectories ultimately bounded. The proposed controller is tested by means of numerical simulations and real–time experiments, which support its practical viability.

1 Introduction

Underactuated mechanical systems are systems which have more degrees-of-freedom than actuators to control. Their uses are common on a lot of applications as robot mobile systems, vehicles used on space or under the sea (with special features that increases difficulties to control) or because of the mathematical model used for control design as where joint flexibility is included in the model. The Furuta pendulum is a well–known underactuated mechanical system used by many control researchers to test linear and non linear techniques[1]. This mechanism consists in an arm rotating in the horizontal plane and pendulum rotating in the vertical plane. The system has only one actuator that provides torque $\tau \in \mathbb{R}$ at the arm.

Feedback linearization is a commonly control technique used in non linear systems; see for example [2]. The basic idea of the feedback linearization control is to define a proper measurable output. Then, by computing an appropriated number of time differentiations of the output, the controller is derived so that the resulting closed–loop system is linear and time–invariant. A possible disadvantage of this approach is that the so–called zero dynamics may be unstable.

The purpose of this document in to introduce a new control scheme which is based in the feedback linearization technique. The control objective is to keep the error trajectories uniformly ultimately bounded. Numerical simulations and real–time experiments support the introduced theory and show its practical viability.

* Work supported by CONACyT, project number 176587, and SIP–IPN, Mexico.
** Author to whom correspondence should be addressed.

Mireya García-Vázquez, Grigori Sidorov (Eds.).
Advances in Computing Science and Control.
Research in Computing Science 59, 2012, pp. 99- 110

The Furuta pendulum dynamics and the control problem formulation are given in Section 2. A new control is proposed in Section 3. There, the closed–loop system and zero dynamics are discussed. In Section 4, by using an original experimental platform which has been accurately identified, the numerical and real–time experimental tests are presented. Finally, some concluding remarks are provided in Section 5.

2 Furuta pendulum dynamic model and control problem formulation

2.1 Model

As previously described, the Furuta pendulum is mechanism consisting in an arm rotating in the horizontal plane and pendulum rotating in the vertical plane. See Figure 1 for a description of the relative joint angle measurements and torque application.

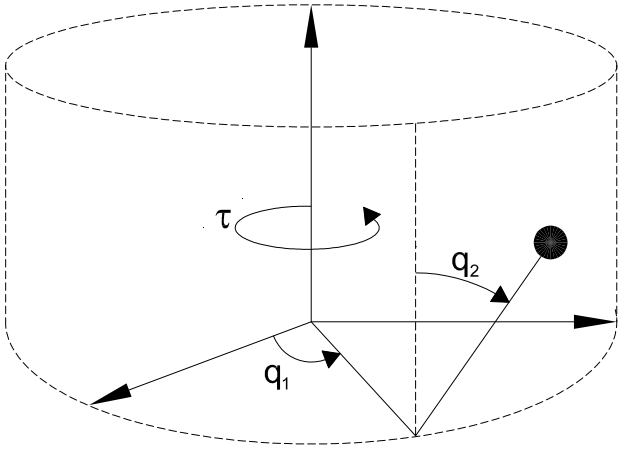

Fig. 1. Furuta pendulum.

The dynamic model of the Furuta pendulum in Euler-Langrange form is written as [1], [4], [5],

$$M(\boldsymbol{q})\ddot{\boldsymbol{q}} + C(\boldsymbol{q}, \dot{\boldsymbol{q}})\dot{\boldsymbol{q}} + \boldsymbol{g}(\boldsymbol{q}) + F_v\dot{\boldsymbol{q}} + \boldsymbol{f}_{cl}(\dot{\boldsymbol{q}}) = \boldsymbol{u}, \tag{1}$$

where

$$\boldsymbol{q} = \begin{bmatrix} q_1 \\ q_2 \end{bmatrix}$$

is the vector of joint position,

$$\boldsymbol{u} = \begin{bmatrix} \tau \\ 0 \end{bmatrix}$$

is the torque input vector, being $\tau \in \mathbb{R}$ the torque input of the arm,

$$M(\boldsymbol{q}) = \begin{bmatrix} \theta_1 + \theta_2 \sin^2(q_2) & \theta_3 \cos(q_2) \\ \theta_3 \cos(q_2) & \theta_4 \end{bmatrix},$$

$$C(\boldsymbol{q}, \dot{\boldsymbol{q}}) = \begin{bmatrix} \frac{1}{2}\theta_2 \dot{q}_2 \sin(2q_2) & -\theta_3 \dot{q}_2 \sin(q_2) + \frac{1}{2}\theta_2 \dot{q}_1 \sin(2q_2) \\ -\frac{1}{2}\theta_2 \dot{q}_1 \sin(2q_2) & 0 \end{bmatrix},$$

$$\boldsymbol{g}(\boldsymbol{q}) = \begin{bmatrix} 0 \\ -\theta_5 \sin(q_2) \end{bmatrix},$$

$$F_v = \begin{bmatrix} f_{v1} & 0 \\ 0 & f_{v2} \end{bmatrix} = \begin{bmatrix} \theta_6 & 0 \\ 0 & \theta_7 \end{bmatrix},$$

$$\boldsymbol{f}_{cl}(\dot{\boldsymbol{q}}) = \begin{bmatrix} f_{c1} \tanh(\beta \dot{q}_1) \\ f_{c2} \tanh(\beta \dot{q}_2) \end{bmatrix} = \begin{bmatrix} \theta_8 \tanh(\beta \dot{q}_1) \\ \theta_9 \tanh(\beta \dot{q}_2) \end{bmatrix},$$

where $M(\boldsymbol{q}) \in \mathbb{R}^{2\times 2}$ is the positive definite inertia matrix and $C(\boldsymbol{q}, \dot{\boldsymbol{q}})\dot{\boldsymbol{q}} \in \mathbb{R}^{2\times 1}$ is the centrifugal and Coriolis torque vector, $\boldsymbol{g}(\boldsymbol{q}) \in \mathbb{R}^{2\times 1}$ is known as the gravitational torque vector, $F_v \in \mathbb{R}^{2\times 2}$ is a diagonal matrix of containing the viscous friction coefficients of each joint, and $\boldsymbol{f}_{cl}(\dot{\boldsymbol{q}}) \in \mathbb{R}^{2\times 1}$ is continuous and differentiable version of the Coulomb friction vector with $\beta > 0$ large enough.

The physical meaning of the input vector $\boldsymbol{u} \in \mathbb{R}^2$ is that the system is equipped with one actuator only, which delivers the torque input $\tau \in \mathbb{R}$.

2.2 Control problem

First, let us define the following signals

$$\boldsymbol{e} = \begin{bmatrix} e_1 \\ e_2 \end{bmatrix} = \begin{bmatrix} q_{d1} - q_1 \\ -q_2 \end{bmatrix} \in \mathbb{R}^2, \tag{2}$$

where $q_{d1}(t)$ is twice differential signal that denotes the desired angle position of the arm.

The control problem consists in designing a controller $\tau \in \mathbb{R}$ such that the error trajectories $\boldsymbol{e}(t) \in \mathbb{R}^2$ satisfies the definition of a uniformly ultimately bounded signal. In other words, the controller should guarantee

$$\|\boldsymbol{e}(0)\| < \alpha \;\; \Rightarrow \;\; \|\boldsymbol{e}(t)\| \leq b \;\; \forall\, t \geq t_0 + T. \tag{3}$$

3 Proposed scheme

3.1 A controller derived from feedback linearization

Let us define the vectors

$$\boldsymbol{h}_v = \begin{bmatrix} h_{v1} \\ h_{v2} \end{bmatrix} = \frac{1}{\det M(q)} \begin{bmatrix} M_{22} z_1 - M_{12} z_2 \\ -M_{21} z_1 + M_{11} z_2 \end{bmatrix}, \tag{4}$$

with

$$z_1 = C_{11}\dot{q}_1 + C_{12}\dot{q}_2 + f_{v1}\dot{q}_1 + f_{c1}\tanh(\beta\dot{q}_1), \tag{5}$$
$$z_2 = C_{21}\dot{q}_1 + C_{22}\dot{q}_2 + g_2 + f_{v2}\dot{q}_2 + f_{c2}\tanh(\beta\dot{q}_2), \tag{6}$$

and

$$\boldsymbol{g}_v = \begin{bmatrix} g_{v1} \\ g_{v2} \end{bmatrix} = \frac{1}{\det M(q)} \begin{bmatrix} M_{22} \\ -M_{21} \end{bmatrix}. \tag{7}$$

Thus, by using the definition of $\boldsymbol{e}$ in (2), the open–loop dynamics can be written as

$$\frac{d}{dt}\begin{bmatrix} e_1 \\ e_2 \end{bmatrix} = \begin{bmatrix} \dot{e}_1 \\ \dot{e}_2 \end{bmatrix}, \tag{8}$$
$$\frac{d}{dt}\begin{bmatrix} \dot{e}_1 \\ \dot{e}_2 \end{bmatrix} = \begin{bmatrix} \ddot{q}_{d1} - h_{v1} - g_{v1}\tau \\ -h_{v2} - g_{v2}\tau \end{bmatrix} \tag{9}$$

Feedback linearization is a control technique commonly used in non linear systems. This approach consists in the transformation of the non linear system into an equivalent system through a proper output signal.

Now, consider

$$\boldsymbol{r} = \dot{\boldsymbol{e}} + \Delta\boldsymbol{e}, \tag{10}$$

where $\Delta = diag\{\Delta_1, \Delta_2\} \in \mathbb{R}^{2\times 2}$ which is positive definite. For the open loop system (8)–(9) we propose the output function

$$y = r_1 + r_2 \tag{11}$$

where r_1 and r_2 are defined in (10).

Equation (11) satisfies

$$\dot{y} = \ddot{e}_1 + \Delta_1\dot{e}_1 + \ddot{e}_2 + \Delta_2\dot{e}_2 \tag{12}$$
$$= \ddot{q}_{d1} - [h_{v1} + h_{v2}] - [g_{v1} + g_{v2}]\tau + \Delta_1\dot{e}_1 + \Delta_2\dot{e}_2 \tag{13}$$

The output equation (11) can be turned into an exponentially convergent signal by using a torque input given by

$$\tau = \tau_{fbl} = \frac{\ddot{q}_{d1} + K_p y - [h_{v1} + h_{v2}] + \Delta_1\dot{e}_1 + \Delta_2\dot{e}_2}{g_{v1} + g_{v2}}, \tag{14}$$

where K_p is a positive constant.

Notice that the controller (14) is valid in a region of the state space where

$$g_{v1} + g_{v2} \neq 0.$$

However, without loss of generality, in this paper we assume that

$$g_{v1} + g_{v2} < 0, \ \forall\, \boldsymbol{q} \in \mathbb{R}^2. \tag{15}$$

Let us notice that the experimental case study presented in this paper satisfies assumption (15); see Section 5.

The closed–loop system can be written as

$$\frac{d}{dt}y = -K_p y, \tag{16}$$

for which we have that

$$\lim_{t\to\infty} y(t) = 0,$$

with exponential convergence rate.

3.2 Zero dynamics

The zero dynamics is obtained assuming that the output signal y and its time–derivative are equal to zero, that is,

$$y = 0, \tag{17}$$

and

$$\dot{y} = 0. \tag{18}$$

In preparation to obtain the zero dynamics, let us first take into account that by virtue of definition (2), the following

$$\begin{aligned} q_1 &= q_{d1} - e_1, \\ \dot{q}_1 &= \dot{q}_{d1} - \dot{e}_1, \\ q_2 &= -e_2, \\ \dot{q}_2 &= -\dot{e}_2, \end{aligned}$$

is satisfied. At the same time

$$\begin{aligned} h_{v1}(q_1, q_2, \dot{q}_1, \dot{q}_2) &= h_{v1}(t, e_1, e_2, \dot{e}_1, \dot{e}_2), \\ h_{v2}(q_1, q_2, \dot{q}_1, \dot{q}_2) &= h_{v2}(t, e_1, e_2, \dot{e}_1, \dot{e}_2), \\ g_{v1}(q_1, q_2) &= g_{v1}(t, e_1, e_2), \\ g_{v2}(q_1, q_2) &= g_{v2}(t, e_1, e_2), \end{aligned}$$

which means that the Furuta pendulum dynamics can be expressed as a function of the time t, the position tracking error $\boldsymbol{e}$, and the velocity tracking error $\dot{\boldsymbol{e}}$.

From the equation (17) and the definition of $\boldsymbol{r}$ in (10), we have that

$$\frac{d}{dt}e_1 + \Delta_1 e_1 = -\frac{d}{dt}e_2 - \Delta_1 e_2 \tag{19}$$

is satisfied.

Besides, by using (18), the fact that

$$\ddot{e}_1 = \ddot{q}_{d1} - \ddot{q}_1 = \ddot{q}_{d1} - h_{v1} - g_{v1}\,\tau\big|_{y=0}\,,$$

expanding the definition of h_{v1} in (4) as

$$h_{v1} = h_{C1} - \frac{\theta_3 \cos(q_2)}{\det(M)}\left[-\theta_5 \sin(q_2)\right]$$

with

$$h_{C1} = \frac{M_{22}}{\det(M)} z_1 - \frac{M_{12}}{\det(M)} \left[C_{21}\dot{q}_1 \right.$$

$$\left. + C_{22}\dot{q}_2 + f_{v2}\dot{q}_2 + f_{c2}\tanh(\beta\dot{q}_2) \right],$$

z_1 in (5), and using the definition $q_2 = -e_2$, it is possible to show that

$$\frac{d^2}{dt^2}e_2 + \kappa(\boldsymbol{q})\Delta_2\frac{d}{dt}e_2 + \kappa(\boldsymbol{q})\frac{\theta_3\cos(q_2)}{\det(M)}\theta_5\sin(e_2) = -\kappa(\boldsymbol{q})[\ddot{q}_{d1} + \Delta_1\dot{e}_1]$$

$$+\kappa(\boldsymbol{q})h_{C1} - \frac{g_{v1}}{g_{v1}+g_{v2}}h_{v2}, \tag{20}$$

where

$$\kappa(\boldsymbol{q}) = \kappa(t,\boldsymbol{e}) = 1 - \frac{g_{v1}}{g_{v1}+g_{v2}}$$

Notice that by virtue of the fact that g_{v1} (see its definition in equation (7)), and the assumption (15), the inequality

$$\kappa(\boldsymbol{q}) > 0,\ \forall\, \boldsymbol{q} \in \mathbb{R}^2,$$

is satisfied.

The system (19) and (20) governs the dynamics of the signals $[e_1\ e_2\ \dot{e}_2]^T \in \mathbb{R}^3$ for $y(t) = \dot{y}(t) = 0$ for all $t \geq 0$, that is, equations (19) and (20) represent a form to describe the zero dynamics.

In agreement with the discussion about the dependency of the Furuta pendulum dynamics, it is clear that

$$\begin{aligned} h_{v1}(t,e_1,e_2,\dot{e}_1,\dot{e}_2) &= h_{C1}(t,e_1,e_2,\dot{e}_1,\dot{e}_2) - \frac{\theta_3\cos(-e_2)}{\det(M)}\left[-\theta_5\sin(-e_2)\right] \\ &= h_{C1}(t,e_1,e_2,\dot{e}_1,\dot{e}_2) - \frac{\theta_3\cos(e_2)}{\det(M)}\left[\theta_5\sin(e_2)\right]. \end{aligned}$$

3.3 Discussion on the control goal

It is possible to show that the trajectories of the zero dynamics (19) and (20) are uniformly ultimately bounded. However, the proof of this fact will be left out for shortening of this paper.

The exponential convergence of the output signal $y(t)$, and the assumption that $q_{d1}(t)$, $\dot{q}_{d1}(t)$, and $\ddot{q}_{d1}(t)$ are bounded, guarantee that the signals $e_1(t)$ and $e_2(t)$ are uniformly ultimately bounded.

Furthermore, there is an ultimate bound of the trajectories $e_1(t)$ and $e_2(t)$ that depends on the Furuta pendulum dynamics and on the control gains Δ_1 and Δ_2.

Fig. 2. Furuta pendulum prototype built at *Instituto Politécnico Nacional–CITEDI* Research Center.

4 Numerical and experimental results

In this section, the real–time implementation of the proposed controller (14) is presented. The experimental tests have been conducted in a Furuta pendulum built at the *Instituto Politécnico Nacional–CITEDI* Research Center. See Figure 2 for picture of the experimental system.

The constant parameters θ_i of the Furuta pendulum model in (1) have been identified by using a procedure based on least squares. These parameters are shown in Table 1, which was obtained by using the filtered dynamic model and the classical least squares identification; see for instance [6] and [7], where identification procedures for mechanical systems are proposed. In the identification process, we considered

$$\beta = 100,$$

which is related to the vector of Coulomb friction $\boldsymbol{f}_{cl}(\dot{\boldsymbol{q}}) \in \mathbb{R}^2$ in the Furuta pendulum model (1).

The identified model was useful to perform numerical simulations of the proposed theory and as previous step to achieve implementations in real–time. Let us notice that

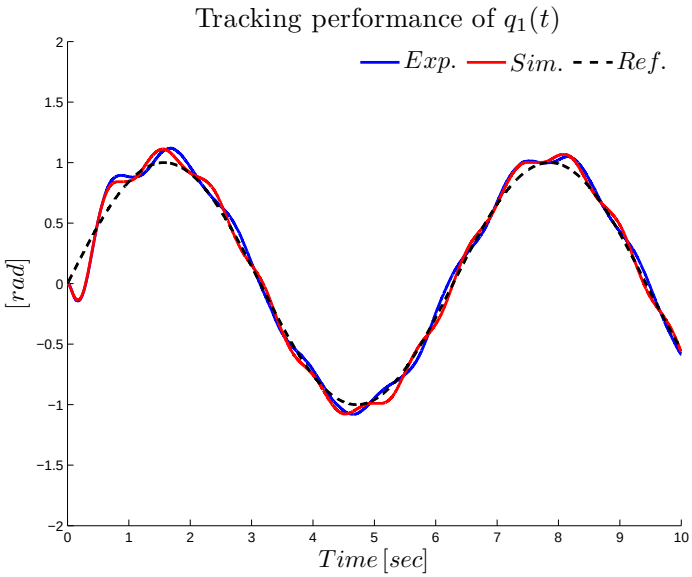

Fig. 3. Simulation and experiment: Time evolution of $q_d(t)$ and $q_1(t)$ obtained by simulation and experiment.

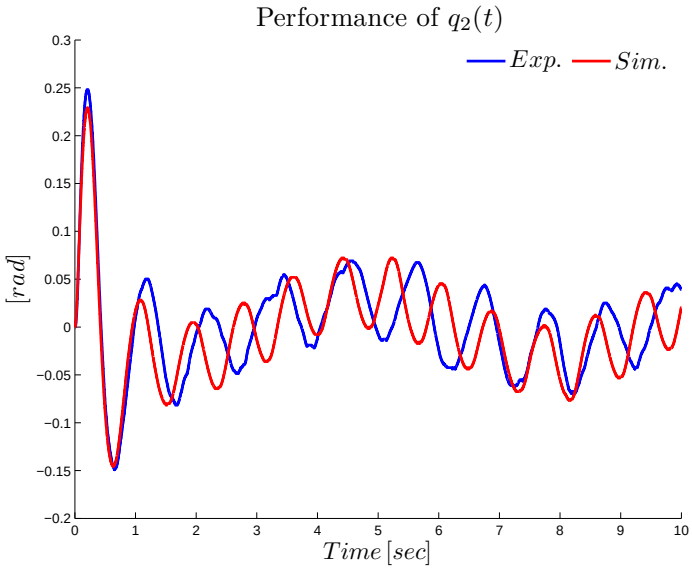

Fig. 4. Simulation and experiment: Time evolution of $q_2(t)$ obtained by simulation and experiment.

Table 1. Numerical values of the Furuta pendulum parameters.

Symbol	Value	Unit
θ_1	0.20959	$\mathrm{Kg}\cdot\mathrm{m}^2\cdot\mathrm{rad}$
θ_2	0.04926	$\mathrm{Kg}\cdot\mathrm{m}^2\cdot\mathrm{rad}$
θ_3	0.06258	$\mathrm{Kg}\cdot\mathrm{m}^2\cdot\mathrm{rad}$
θ_4	0.04539	$\mathrm{Kg}\cdot\mathrm{m}^2\cdot\mathrm{rad}$
θ_5	1.71142	$\mathrm{Kg}\cdot\mathrm{m}^2\cdot\mathrm{rad}$
θ_6	0.08514	$\mathrm{N}\cdot\mathrm{m}\cdot\mathrm{rad/sec}$
θ_7	0.00238	$\mathrm{N}\cdot\mathrm{m}\cdot\mathrm{rad/sec}$
θ_8	0.13738	$\mathrm{N}\cdot\mathrm{m}\cdot\mathrm{rad/sec}$
θ_9	0.02789	$\mathrm{N}\cdot\mathrm{m}\cdot\mathrm{rad/sec}$

to obtain a successful experimental result the applied torque should respect the power limits. Besides, simulations are important to check that stability is still obtained in spite of the fact that the controller is implemented in discrete form and the joint velocity is estimated through discrete differentiation from joint position measurements.

Since the experimental system has been identified, experiments have been compared with respect to numerical simulations.

The desired joint position trajectory $q_{d1}(t)$ for the arm position was defined as

$$q_{d1}(t) = 1.0\sin(t)$$

Besides, concerning the output function y in (11), we used

$$\Delta_1 = 5.0, \tag{21}$$

$$\Delta_2 = 8.0. \tag{22}$$

and $K_p = 10.0$ in the new controller (14).

The initial condition of the experimental system was

$$\begin{bmatrix} q_1(0) \\ q_2(0) \end{bmatrix} = \begin{bmatrix} 0 \\ 0 \end{bmatrix} \ [\mathrm{rad}],$$

and

$$\begin{bmatrix} \dot{q}_1(0) \\ \dot{q}_2(0) \end{bmatrix} = \begin{bmatrix} 0 \\ 0 \end{bmatrix} \ [\mathrm{rad/s}].$$

4.1 Results

The numerical and experimental results are illustrated in Figures 3–6. In particular, the Figure 3 shows the time evolution of $q_{d1}(t)$ and $q_1(t)$, and the Figure 4 depicts the time evolution of $q_2(t)$. The applied torque $\tau(t)$ and the output signal $y(t)$ are observed in Figures 5 and 6, respectively.

As observed in Figures 3–6, the experimental results and the simulation are very similar, which shows that the identified parameters θ_i are relatively accurate.

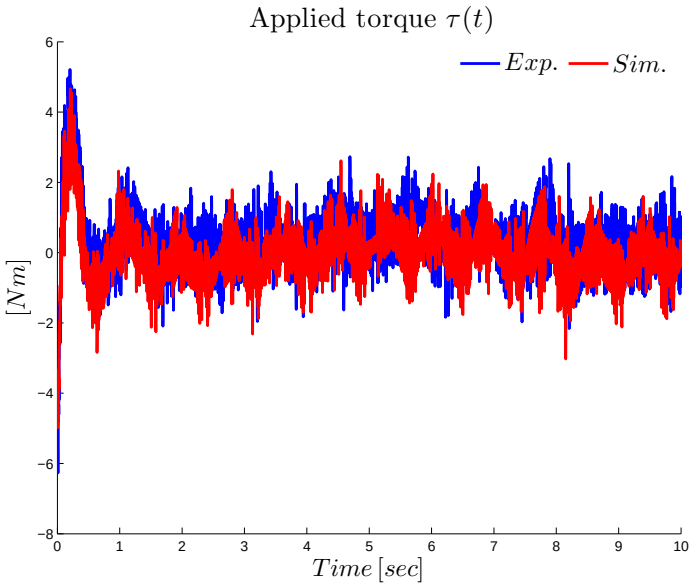

Fig. 5. Simulation and experiment: Time evolution of control input $\tau(t)$.

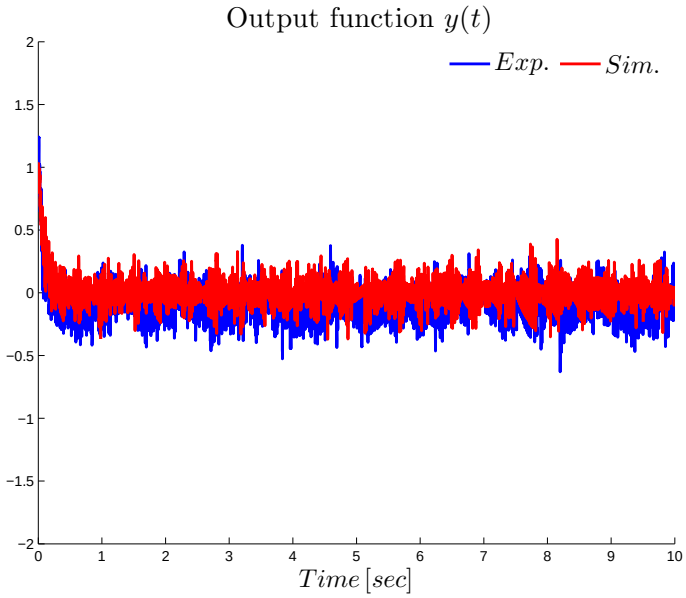

Fig. 6. Simulation and experiment: Time evolution of the output signal $y(t)$.

The control action $\tau(t)$ obtained by simulation and experiment has high frequency components. This is attributed to the velocity estimation obtained by using the dirty derivative algorithm [8]

$$\dot{\boldsymbol{q}}(Tk) \approx \frac{\boldsymbol{q}(Tk) - \boldsymbol{q}(T[k-1])}{T}, \tag{23}$$

with $T = 0.001$ [s] the sampling period and k the integer time index, and the PWM switching of the servo amplifier.

Also, in Figure 6 the response of the output function $y(t)$ in (11) is appreciated for both simulation and experiment. Although theory predicts exponential convergence of $y(t)$, an oscillatory behavior with high frequency components is presented. It is noteworthy that the output function $y(t)$ in (11) depends of the joint velocity $\dot{\boldsymbol{q}}(t) \in \mathbb{R}^2$. The main reason for the oscillatory behavior of $y(t)$ is that the joint velocity $\dot{\boldsymbol{q}}(t)$ is estimated via the noisy dirty derivative algorithm (23) and the relative high value of the gains Δ_1 and Δ_2 in (21) and (22), respectively.

By means of numerical simulation assuming a continuous time implementation of the controller and non quantized position and velocity measurements, the exponential convergence of $y(t)$ was corroborated

5 Concluding remarks

A new controller based on the feedback linearization technique has been introduced in this paper.

The output function $y(t)$ was selected as a linear combination of the position and velocity tracking errors. In fact, the output function $y(t)$ is inspired from the filtered tracking error used in passivity–based controllers for fully actuated mechanical systems; see [3] for example.

The main result consisted in proving that the output function converges to zero in an exponential form, while the trajectories of the zero dynamics are uniformly ultimately bounded. Simulations and real–time experiments confirmed the validity of the main result.

Current work is focused in the application of the proposed ideas to other under actuated mechanical systems. Other possible extension is the use of integral action to define the output function $y(t)$. The addition of integral action can induce the behavior of second order system in the time evolution of the output function $y(t)$. However, this idea is also under research.

References

1. I. Fantoni and R. Lozano, *Non–Linear Control for Underactuated Mechanical Systems*, Springer–Verlag, London, 2002.
2. H. K. Khalil, *Nonlinear Systems*, Prentice Hall, Upper Saddle River, 1996.
3. A. Behal, W. E. Dixon, B. Xian, and D. M. Dawson, *Lyapunov-Based Control of Robotic Systems*, Taylor and Francis, 2009,

4. L. Sciavicco and B. Siciliano, *Modelling and Control of Robot Manipulators*, Springer–Verlag, London, 2000.
5. B. S. Cazzolato and Z. Prime, "On the dynamics of the furuta pendulum", *Journal of Control Science and Engineering*, Vol. 2011, Article ID 528341, 8 pages.
6. P. Logothetis and J. Kieffer, "On the identification of the robot dynamics without acceleration measurements", Internal Report, Faculty of Engineering and Information Technology, Australian National University, 1996. Available at `http://citeseerx.ist.psu.edu/viewdoc/summary?doi=10.1.1.55.8716`
7. M. Gautier and Ph. Poignet, "Extended Kalman filtering and weighted least squares dynamic identification of robot", *Control Engineering Practice*, Vol 9, No. 12, pp. 1361–1372, 2001.
8. R. Kelly, V. Santibáñez and A. Loria, *Control of Robot Manipulators in Joint Space*, Springer–Verlag, London, 2005.